Available online at www.sciencedirect.com
ScienceDirect
Journal of Sound and Vibration 300 (2007) 101–116
JOURNAL OF SOUND AND VIBRATION
www.elsevier.com/locate/jsvi

Optimisation of a resonance changer to minimise the vibration transmission in marine vessels

Paul G. Dylejko[a,*], Nicole J. Kessissoglou[a], Yan Tso[b], Chris J. Norwood[b]

[a]*School of Mechanical and Manufacturing Engineering, The University of New South Wales, Sydney, NSW 2052, Australia*
[b]*Defence Science and Technology Organisation (DSTO), Maritime Platforms Division, Fishermans Bend, Vic. 3207, Australia*

Received 2 December 2005; received in revised form 7 June 2006; accepted 24 July 2006
Available online 27 October 2006

Abstract

Structure-borne noise generated by marine vessels is an area that receives much research attention. Significant noise levels are generated due to onboard machinery such as the diesel engines, gearboxes, generators, and auxiliary machinery. In the case of ships and submarines, a major source of the radiated noise at low frequencies is due to excitation of the hull modes resulting from vibration transmission through the propeller-shafting system. Oscillations occur at the propeller due to small variations in thrust when the propeller blades rotate through the non-uniform wake, resulting in axial excitation of the propeller at the blade pass frequency. This problem can be addressed by the use of a resonance changer (RC) which performs the task of a hydraulic dynamic vibration absorber, thereby reducing the vibration transmission and avoiding excitation of hull axial resonances. This research is concerned with optimisation of both single and dual RC configurations in a submarine. An optimisation scheme involving a genetic and a general nonlinear constrained algorithm is used to minimise two fitness functions associated with the vibration transmission to the hull over a low-frequency range. The dynamic response of the propeller-shafting system is characterised using the transmission matrix approach. This modular description enables greater flexibility for dynamic modelling of the propeller-shafting system, and can be easily manipulated for future design modifications.

1. Introduction

It is desirable to minimise the vibro-acoustic responses of maritime vessels to improve passenger comfort, minimise crew fatigue, and in the case of naval vessels, to avoid detection. Oscillations of onboard equipment such as the diesel engines and the propulsion system generates significant vibration that propagates through the supporting structure to the hull, where it is radiated as structure-borne noise. The vibration transmission through the propeller-shafting system of ships and submarines represents a critical issue that must be addressed in order to reduce the low-frequency acoustic signature. The propeller-shafting system can be simplified into the key features shown in Fig. 1. Axial excitation of the propeller occurs at low frequencies due to the non-uniform wake velocity caused by asymmetry in the hull or protrusions of control surfaces. The

*Corresponding author. Tel.: +61 3 9626 8218; fax: +61 3 9626 8373.
E-mail address: paul.dylejko@dsto.defence.gov.au (P.G. Dylejko).

0022-460X/$ - see front matter © 2006 Elsevier Ltd. All rights reserved.
doi:10.1016/j.jsv.2006.07.039

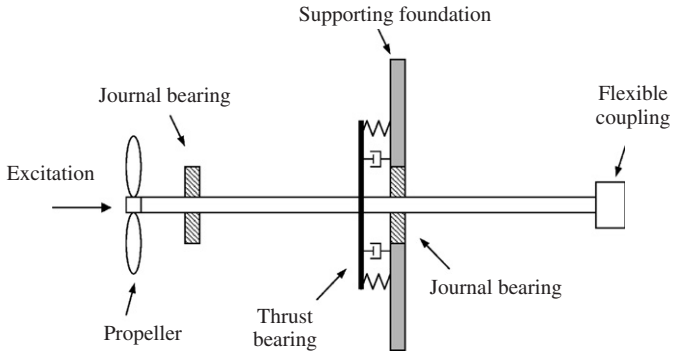

Fig. 1. Simplified representation of the propeller-shafting system [1].

oscillations which occur at the propeller are the result of small variations in thrust when the propeller blades rotate through the non-uniform wake. The frequency of these oscillations is at the blade pass frequency (rotational speed of the shaft multiplied by the number of blades on the propeller). The disturbances at the propeller result in vibration transmission through the propeller-shafting system and subsequent axial excitation of the hull. The engine also introduces excitation to the propeller-shafting system; however, it is assumed that this is essentially isolated by the flexible coupling which limits the influence of the engine side from the propeller side of the propulsion system [1]. Development of propeller-shafting models for maritime vessels has been undertaken by numerous researchers [1–3]. In most of these studies, the aim has been to reduce the axial vibration and its transmission into the hull. A detailed paper by Goodwin [2] examined the reduction of excessive vibration through the propeller-shafting system by using an existing hydraulic device called the "Michell Thrustmeter". This device is located in series between the thrust bearing and supporting foundation and is used to measure the thrust which is transmitted to the vessel from the propeller-shafting system. Goodwin adapted and redesigned the Michell Thrustmeter to reduce the vibration transmission through the propeller-shafting system. For this new application, the device was known as a resonance changer (RC), also known as a detuner. The RC introduces virtual elastic, damping and inertial influences by hydraulic means, thereby acting as a dynamic vibration absorber (DVA). The simplified model of the RC introduced by Goodwin is shown in Fig. 2. The RC consists of a piston of cross-sectional area A_0, an oil reservoir of volume V_1 and a pipe connecting these two elements of length L_1 and cross-sectional area A_1. Goodwin examined the reduction of the force transmissibility using a simplified spring–mass model of the propeller-shafting system. Reduction of the force transmissibility was achieved by firstly tuning the natural frequency of the RC to that of the propeller-shafting system's natural frequency and then optimising the RC's damping rate. Goodwin also offered insight into design values for the RC's mass and stiffness. The performance of the RC during sea trials exceeded expectations, eliminating the resonance conditions suffered previously. Although the paper by Goodwin is comprehensive in all practical respects, a relatively simple model of the propeller-shafting system was used and the coupling with the hull was not included.

A RC is essentially a hydraulic DVA, where a DVA is a spring–mass–damper device attached to a "primary" physical system with the aim of reducing its response. Frahm is acknowledged to have invented the DVA in 1911 [4]. Early work on DVAs concentrated on tuning the undamped DVA to the frequency of the harmonic excitation acting on the primary system. This type of absorber exhibits good performance over a narrow frequency bandwidth; however, it becomes inefficient as the disturbing frequency shifts. The addition of damping alleviates the narrow band characteristics of the undamped DVA. DVAs have been utilised extensively to reduce vibrations in various types of machinery and structures [5–12]. Much work has been completed on the optimisation of DVAs attached to different structures. Hartog [7] analytically investigated the design of DVAs for use with single degree-of-freedom (dof) systems by obtaining optimal values of the absorber spring, mass and damping constants. This analysis however was restricted to primary systems that did not exhibit damping.

A simple method that has been used to optimise the response of a primary system with an attached DVA is the single-dof method. The response of a single resonance is minimised in this method by ignoring the response

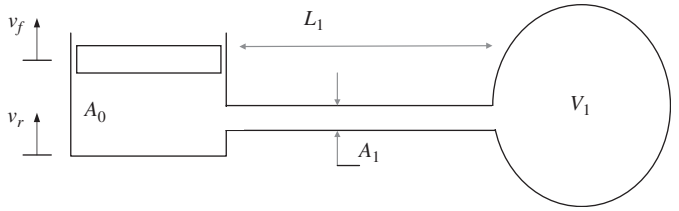

Fig. 2. Simplified model of the resonance changer [2].

outside the influence of the chosen resonance. The application of DVAs is not restricted to lumped parameter systems, Neubert [8] used the single-dof method technique to reduce the axial response of a bar at a chosen resonance frequency. Mobility was used to characterise the dynamic response of the structure. A method for the efficient reduction of the dynamic response of large-scale multi-dof systems subject to harmonic excitation using multiple DVAs was reported by Kitis et al. [9]. The reduction in computational expense reported in their work was achieved by using a re-analysis technique for computing the cost function and its derivatives. The benefit associated with this technique is that the complete structural analysis is performed only once. Subsequent calculation of the cost function and its derivatives only require the solution of a set of linear algebraic equations. The vibratory response over a frequency range of a cantilever beam approximated by 22-dof with two attached DVAs was then minimised. While the majority of research has been concerned with examining the dynamic response in the frequency domain, DVAs have been utilised to improve the response in the time domain as well. Lau and Lam [10] examined both time and frequency domain response optimisation using four different methods for a single-dof system with primary damping. These methods included the equal peak method, the minimal variance method, the energy method and the area ratio method. It was found that time domain optimisation was best suited for reduction of the transient response. Rice [11] examined the use of multiple DVAs to reduce the maximum response of a continuous system over a frequency range. The primary system was characterised using modal data. A numerical optimisation of the parameters and positioning of the multiple DVAs was performed using the SIMPLEX algorithm. Work by Rade and Steffen [12] involved solving a general nonlinear constrained optimisation problem to obtain the DVA parameters which resulted in the minimum response of a continuous system over multiple frequency bands. A substructure coupling technique was used to characterise the frequency response function of the combined system. The influence of perturbations in the DVAs parameters was also examined.

In this paper, the transmission matrix method, also known as the four-pole parameter method is used to model the low-frequency dynamic response of the propeller-shafting system in a submarine. Two fitness functions associated with the vibration transmission to the hull over a low-frequency range as a function of the RC parameters are developed. Both fitness functions are minimised using a genetic and a general nonlinear constrained algorithm within realistic constraints, resulting in optimal values for the virtual RC parameters. The results obtained using the different fitness functions are presented for both single and dual RC configurations. The subsequent advantages of the different fitness functions and number of RCs are discussed. A perturbation analysis on the RC parameters is also presented and the effects on the RC performance are observed.

2. Transmission matrix model of the dynamic system

Due to the symmetry of the geometry and loading of the propeller-shafting system in a submarine, the transmission matrix method [13,14] has been chosen to characterise the dynamic response. A transmission matrix schematic of the propeller-shafting system is given in Fig. 3. The mechanical components have been broken down into subsystems to enable a modular description of the complete system's dynamic response. The proposed dynamic model assumes that the propeller and the entrained water around the propeller are represented as a lumped mass of mass m_p with viscous damping c_p. The propeller is attached to a continuous model of the shaft consisting of cross-sectional area A_s, Young's modulus E_s and density ρ_s. Since the response at a point along the shaft corresponding to the location of the thrust bearing is desired, an effective length l_{se} is

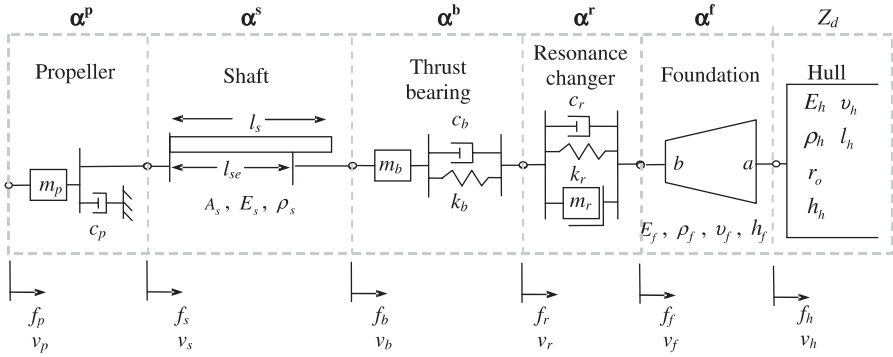

Fig. 3. Transmission matrix representation of propeller-shafting model connected to the submarine hull.

defined. The thrust bearing is represented by a linear stiffness k_b, damping coefficient c_b and mass m_b. The RC exhibits inertial, elastic and damping properties, represented by m_r, k_r and c_r, respectively. Referring to Fig. 2, these virtual mass, stiffness and damping parameters can be expressed by [2]

$$m_r = \frac{\rho_1 A_0^2 L_1}{A_1}, \tag{1}$$

$$k_r = \frac{A_0^2 B_1}{V_1}, \tag{2}$$

$$c_r = 8\pi\mu_1 L_1 \frac{A_0^2}{A_1^2}. \tag{3}$$

These parameters are associated with the force required to overcome the inertia of the oil in the pipe, compress the oil in the reservoir and overcome the viscous resistance of the oil in the pipe. ρ_1, μ_1 and B_1 are, respectively, the density, viscosity and bulk modulus of the oil contained within the RC system. The thrust block is coupled to the hull via a truncated conical shell foundation. E_f, ρ_f, ν_f, h_f, respectively, represent Young's modulus, density, Poisson's ratio and thickness of the foundation. The radii of the major and minor base of the conical shell are a and b, ϕ is the semivertex angle. E_h, ρ_h, ν_h, r_o, h_h, A_h and l_h represent Young's modulus, density, Poisson's ratio, outside radius, thickness, cross-sectional area and length of the cylindrical hull, respectively. The velocities at the propeller, shaft, thrust bearing, RC, foundation and hull are described by v_p, v_s, v_b, v_r, v_f and v_h, respectively, while the forces at the previous locations are given by f_p, f_s, f_b, f_r, f_f and f_h.

2.1. Propeller-shafting system

The transmission matrix parameters of the propeller (ignoring the damping due to the surrounding fluid) and shaft are, respectively, given by

$$\boldsymbol{\alpha}^p = \begin{bmatrix} 1 & \mathrm{j}\omega m_p \\ 0 & 1 \end{bmatrix}, \tag{4}$$

$$\boldsymbol{\alpha}^s = \begin{bmatrix} \cos k_s l_{se} & \mathrm{j}\dfrac{A_s E_s k_s \sin k_s l_s}{\omega \cos k_s (l_s - l_{se})} \\ \mathrm{j}\omega \dfrac{\cos k_s (l_s - l_{se}) - \cos k_s l_s \cos k_s l_{se}}{A_s E_s k_s \sin k_s l_s} & \dfrac{\cos k_s l_s}{\cos k_s (l_s - l_{se})} \end{bmatrix}. \tag{5}$$

The shaft transmission matrix parameters were obtained by manipulating the receptance matrix for a free–free rod undergoing longitudinal vibration [15]. $k_s = \omega/c_{Ls}$ is the longitudinal wavenumber, and $c_{Ls} =$

$\sqrt{E_s/\rho_s}$ is the longitudinal wave speed of the shaft. The transmission matrix parameters of the thrust bearing and RC are respectively expressed as

$$\boldsymbol{\alpha}^b = \begin{bmatrix} 1 - \dfrac{\omega^2 m_b}{k_b + \mathrm{j}\omega c_b} & \mathrm{j}\omega m_b \\ \dfrac{\mathrm{j}\omega}{k_b + \mathrm{j}\omega c_b} & 1 \end{bmatrix}, \tag{6}$$

$$\boldsymbol{\alpha}^r = \begin{bmatrix} 1 & 0 \\ \dfrac{j\omega}{k_r + j\omega c_r - \omega^2 m_r} & 1 \end{bmatrix}. \tag{7}$$

2.2. Foundation

A simplified model of a truncated conical shell has been used to model the foundation of the propeller-shafting system in a submarine. It is assumed that the axisymmetric response of the foundation in the low-frequency range can be approximated using membrane theory. The governing equations can be written as [16]

$$U = \cos\phi(\cos^2\phi - \Omega^2\xi^2)^{-1} [(v_f \tan\phi/2\pi E_f h_f)F - (1 - \Omega^2\xi^2)u], \tag{8}$$

$$N_\theta = (E_f h_f/a)(\Omega^2\xi/\sin\phi\cos\phi)[u\cos\phi + U], \tag{9}$$

$$\mathrm{d}F/\mathrm{d}\xi = -2\pi E_f h_f \Omega^2 \xi U \cos\phi, \tag{10}$$

$$\mathrm{d}u/\mathrm{d}\xi = -(E_f h_f \sin\phi)^{-1}[F/2\pi\xi\cos\phi + vaN_\theta]. \tag{11}$$

The geometric parameters and coordinate system of the truncated conical shell used in Eqs. (8) to (11) are shown in Fig. 4. U is the axial displacement of a shell cross section, N_θ is the circumferential stress resultant, u is the displacement of the shell in the meridional direction and F is the total axial force transmitted through a shell cross section. The dimensionless coordinate of the conical shell is: $\xi = s/s_1$, where s is the meridional coordinate of the conical shell (distance measured from apex) and s_1 is the meridional distance from the apex to the major base. The completeness parameter is defined as $\gamma = b/a$. The dimensionless frequency parameter Ω is given by $\Omega = \omega/\omega_0$ where $\omega_0^2 = E_f/\rho_f a^2$.

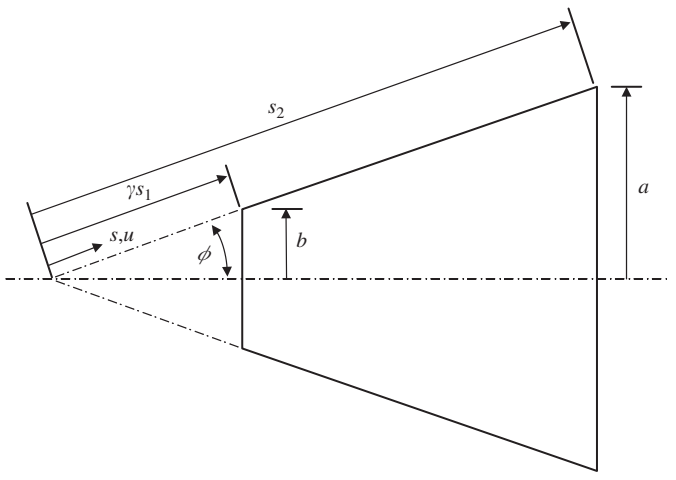

Fig. 4. Coordinate system used with the conical shell model of the foundation.

The four-pole parameters can be found by numerical integration of the second-order equations for two sets of initial conditions at the minor base of the conical shell ($\xi = \gamma$), corresponding to $(F, U) = (1, 0)$ and (0, 1). Using these initial conditions and integrating the differential equations to the major base of the conical shell ($\xi = 1$), results in two sets of influence coefficients, (ψ_{11}, ψ_{21}) and (ψ_{12}, ψ_{22}). The transmission matrix of the foundation is then given by

$$\alpha^f = \begin{bmatrix} \psi_{22} & -\mathrm{i}\psi_{12}/\omega \\ \mathrm{i}\omega\psi_{21} & \psi_{11} \end{bmatrix}. \tag{12}$$

It is important to note that the geometry of the conical shell used by Hu and Kana [16] has been inverted to correspond to the geometry of the foundation shown in Fig. 4.

2.3. Hull

As an initial approximation, the submarine hull was modelled as a one-dimensional rod undergoing axial excitation. It should be noted that this description does not include radial motion of the hull or the subsequent effects of radiation loading. Lumped masses have been added to both ends of the rod to represent the main ballast tank and casing. The transmission matrix parameters associated with the lumped masses and the cylindrical hull are, respectively, given by

$$\boldsymbol{\alpha}^l = \begin{bmatrix} 1 & \mathrm{j}\omega m_l \\ 0 & 1 \end{bmatrix}, \tag{13}$$

$$\boldsymbol{\alpha}^h = \begin{bmatrix} \cos k_h l_h & \mathrm{j}\dfrac{A_h E_h k_h}{\omega}\sin k_h l_h \\ \mathrm{j}\dfrac{\omega}{A_h E_h k_h}\sin k_h l_h & \cos k_h l_h \end{bmatrix}. \tag{14}$$

m_l represents the lumped masses added to the fore and aft of the hull, $k_h = \omega/c_{Lh}$ is the longitudinal wavenumber and $c_{Lh} = \sqrt{E_h/\rho_h}$ is the longitudinal wave speed of the hull. ρ_h is the density of the hull adjusted using Archimedes principle to maintain neutral buoyancy and is defined as

$$\rho_h = \frac{\pi r_o^2 l_h \rho_w - 2m_l}{A_h l_h}, \tag{15}$$

where ρ_w is the density of the surrounding fluid.

The complete hull response $\boldsymbol{\beta}^h$ is the product of the transmission matrices associated with the cylindrical rod and lumped masses:

$$\boldsymbol{\beta}^h = \boldsymbol{\alpha}^l \boldsymbol{\alpha}^h \boldsymbol{\alpha}^l. \tag{16}$$

The resulting axial driving point impedance subject to a free end can be described by [13]

$$Z_d = \frac{\beta_{12}^h}{\beta_{22}^h}, \tag{17}$$

where β_{12}^h and β_{22}^h, respectively, represent the second element in the first and second rows of the matrix $\boldsymbol{\beta}^h$.

2.4. Force and power transmission through the propeller-shafting system

For N number of RCs in series, the combined response of the complete propeller-shafting system $\boldsymbol{\beta}^{ps}$ is given by the forward matrix multiplication of the respective four-pole parameters of the subsystems:

$$\boldsymbol{\beta}^{ps} = \boldsymbol{\alpha}^p \boldsymbol{\alpha}^s \boldsymbol{\alpha}^b \prod_{q=1}^{N} \boldsymbol{\alpha}_q^r \boldsymbol{\alpha}^f. \tag{18}$$

The force at the hull resulting from a unit load at the propeller ($f_p = 1$) is defined by [13]

$$f_h = \left(\beta_{11}^{ps} + \frac{\beta_{12}^{ps}}{Z_d}\right)^{-1}. \tag{19}$$

β_{11}^{ps} and β_{12}^{ps} represent the first and second elements in the first row of the matrix $\boldsymbol{\beta}^{ps}$. The force transmissibility T_F through the propeller-shafting system is given by $T_F = |f_h|$.

The power transmission to the hull has also been examined due to the fact that the hull velocity has a closer direct correlation to the radiated sound pressure. The velocity at the hull arising from a unit load at the propeller is defined by

$$v_h = (\beta_{11}^{ps} Z_d + \beta_{12}^{ps})^{-1}. \tag{20}$$

The time-averaged power transmission to the hull resulting from a unitary harmonic load at the propeller can be expressed as [17]

$$\langle \Pi \rangle = \tfrac{1}{2}\mathrm{Re}(f_h^* v_h), \tag{21}$$

where the brackets $\langle\rangle$ represent time averaged and f_h^* is the complex conjugate of f_h.

3. Optimisation of the RC parameters

3.1. Development of fitness criteria

The force which acts on the propeller in a marine vessel has been shown to be approximately proportional to the propeller rotational speed squared [1,2]. This relationship has been accounted for by weighting the force transmissibility and time-averaged power transmission by the frequency ratio $\omega_i/\Delta\omega$ squared and raised to the fourth power respectively. ω_i is the discrete frequency in the frequency band of interest and $\Delta\omega$ is the frequency bandwidth used in the optimisation. The weighted force transmissibility and weighted time-averaged power transmission at the ith discrete frequency can be, respectively, expressed as

$$T_{F,W}(\omega_i) = \left(\frac{\omega_i}{\Delta\omega}\right)^2 T_F(\omega_i), \tag{22}$$

$$\langle \Pi_W(\omega_i) \rangle = \left(\frac{\omega_i}{\Delta\omega}\right)^4 \langle \Pi(\omega_i) \rangle. \tag{23}$$

It should be noted that these terms do not represent physical quantities. They are, however, suitable for measuring the reduction in force transmissibility or time-averaged power transmission. The fitness criteria to be minimised are the maximum value of the weighted force transmissibility ($J_{T_{F,W}}$) and the maximum value of the weighted time-averaged power transmission ($J_{\langle \Pi_W \rangle}$) and are given by

$$J_{T_{F,W}}(\mathbf{x}) = 20\log_{10}\left\{\max_{\omega_l \leqslant \omega_i \leqslant \omega_u} T_{F,W}(\mathbf{x}, \omega_i)\right\}, \tag{24}$$

$$J_{\langle \Pi_W \rangle}(\mathbf{x}) = 10\log_{10}\left\{\max_{\omega_l \leqslant \omega_i \leqslant \omega_u} \langle \Pi_W(\mathbf{x}, \omega_i) \rangle\right\}. \tag{25}$$

The frequency range included in Eqs. (24) and (25) is bound by lower (ω_l) and upper (ω_u) limits. $\mathbf{x}$ is a vector containing the virtual mass, stiffness and damping parameters associated with the N RCs and is given by:

$$\mathbf{x} = \{\, k_{r,1} \quad m_{r,1} \quad c_{r,1} \quad k_{r,2} \quad m_{r,2} \quad c_{r,2} \quad \ldots \quad k_{r,N} \quad m_{r,N} \quad c_{r,N} \,\}^{\mathrm{T}}. \tag{26}$$

3.2. Genetic algorithm-based optimisation

Only the low-frequency range (<100 Hz) is of interest due to the excitation of the propeller occurring at the blade pass frequency. Lower ($\mathbf{x}_l$) and upper ($\mathbf{x}_u$) limits are also enforced on the RC parameters, that is, $\mathbf{x}_l \leqslant \mathbf{x} \leqslant \mathbf{x}_u$. These two conditions require the use of a constrained optimisation technique. There are numerous optimisation techniques available to solve the constrained fitness criteria defined in the previous section. Many of these techniques are robust but sometimes fail to find the global optimum. Complex fitness functions such as those defined in Eqs. (24) and (25) may contain several local optima. Since a mathematical condition defining the best solution for these cases does not exist, finding this global optimum is usually more computationally involved. One method that has been frequently used by researchers to solve various nonlinear optimisation problems is the genetic algorithm or GA [18,19]. GAs are an artificial application of Darwin's notion of natural selection and evolution, and have been proven to provide robust and accurate solutions to these problems. While equality constraints can be included in the system model, inequality constraints cannot be directly enforced by the GA. The simplest way of applying constraints is by eliminating strings which violate any of the constraints. This method is not ideal since no information is obtained from infeasible solutions. In order to overcome this problem, the penalty method can be used. This method reduces the fitness of the string relative to the constraint violation. Given the constrained optimisation problem: minimise $J(\mathbf{x})$, subject to $h_p(\mathbf{x}) \leq 0$ for $p = 1, 2, ..., n$ where n is the number of constraints, the penalty method transforms the problem into an unconstrained problem suitable for solution by the GA [19]:

$$\text{minimise } J(\mathbf{x}) + \sum_{p=1}^{n} \Phi[h_p(\mathbf{x})], \tag{27}$$

where Φ is the penalty function which is equal to zero when no constraints are violated. A simple penalty function that has been used extensively is the square of the constraint violation multiplied by a penalty coefficient (P) and is given by [19]: $\Phi[h_p(\mathbf{x})] = Ph_p^2(\mathbf{x})$. A dynamic penalty function presented by Erbatur et al. [20] has been used, which adjusts the intensity of the penalty parameter with increasing generations: $\Phi[h_p(\mathbf{x})] = PG^2 h_p(\mathbf{x})$. G represents the generation count. In order to provide a fair penalty distribution, the constraints have been normalised by using

$$h_p(x_p) = \begin{cases} \dfrac{x_{l,p} - x_p}{x_{m,p}}, x_p < x_{l,p}, \\ \dfrac{x_p - x_{u,p}}{x_{m,p}}, x_p > x_{u,p}, \\ 0, x_{l,p} \leqslant x_p \leqslant x_{u,p}, \end{cases} \tag{28}$$

where $x_{m,p} = (x_{l,p} + x_{u,p})/2$. The index p in this case represents the pth element in the respective vector. This normalisation results in three constraints for each RC. Combining this method and the penalty function given above, the cost functions defined in Eqs. (24) and (25) are penalised by adding the following term: Penalty $= PG^2 \sum_{p=1}^{3N} h_p(x_p)$. Values for P of 2.5 and 2.5×10^{-10} have been, respectively, used when considering the force transmissibility and time-averaged power transmission [20].

4. Results

An optimisation scheme utilising a genetic and a general nonlinear constrained algorithm has been used to minimise the fitness criteria defined in Eqs. (24) and (25). The genetic algorithm was used to approximately find the global optima, while the general nonlinear constrained algorithm improved the accuracy of the approximate solution found by the GA. The physical values associated with the propeller-shafting system, foundation and hull used in the modelling are presented in Tables 1–3, respectively. The lumped masses added to the fore and aft of the cylindrical hull were 200 tonnes. The density of the surrounding fluid is assumed to be 1000 kg/m^3. The four-pole parameters of the conical shell obtained from the numerical integration of Eqs. (8)–(11) are given in Fig. 5. Hysteretic damping was included in the shaft and hull by using a complex Young's modulus $E(1 + j\eta)$, where $\eta = 0.02$ is the structural loss factor. The constraints imposed on the RC

Table 1
Propeller-shafting system parameters

Parameter	Value
m_p (tonnes)	10
E_s (GPa)	200
ρ_s (tonnes/m^3)	7.8
A_s (m^2)	0.707
l_s (m)	10.5
l_{se} (m)	9
m_b (tonnes)	0.2
k_b (MN/m)	20000
c_b (tonnes/s)	300

Table 2
Foundation parameters

Foundation parameter	Value
a (mm)	1250
b (mm)	520
ρ_f (kg/m^3)	7700
E_f (GPa)	200
υ_f	0.3
h_f (mm)	10
ϕ (deg)	15

Table 3
Hull parameters

Parameter	Value
E_h (GPa)	200
r_o (m)	3.25
h_h (mm)	45
l_h (m)	60

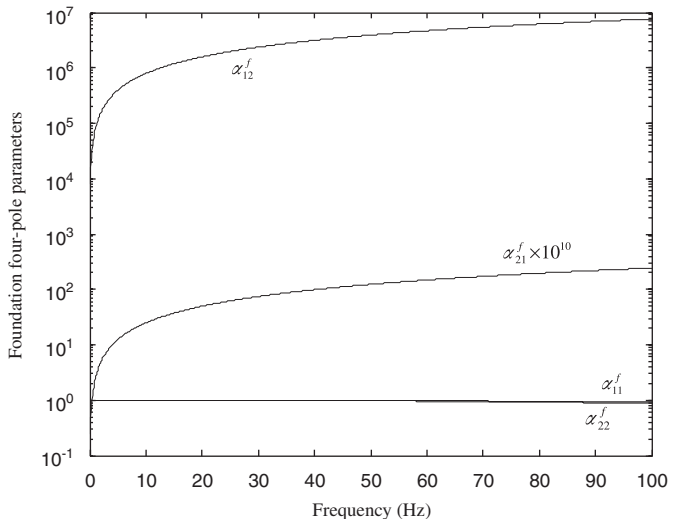

Fig. 5. Four-pole parameters of the foundation $\boldsymbol{\alpha}^f$.

Table 4
Optimisation limits and for the RC parameters

RC parameter	Lower limit	Upper limit
k_r (MN/m)	15	1500
m_r (tonnes)	1	20
c_r (tonnes/s)	5	1100

Table 5
Optimal parameters for a single RC configuration

RC parameter	opt($J_{T_{F,W}}$)	opt($J_{\langle \Pi_W \rangle}$)
k_r (MN/m)	168.51	145.95
m_r (tonnes)	1	1
c_r (tonnes/s)	287.43	67.313

parameters within the optimisation process are shown in Table 4. Minimisation of the maximum weighted force transmissibility and the maximum weighted time-averaged power transmission to the hull have been examined numerically in the following sections. The low-frequency range up to 100 Hz using a frequency increment of 0.01 Hz has been considered. Results obtained using the method outlined by Goodwin [2] for optimisation of the RC parameters are also presented for comparison.

Using a single RC configuration, the optimal values for the RC virtual mass, stiffness and damping parameters are obtained by optimising the fitness criteria given by Eqs. (24) and (25). These two fitness criteria correspond to minimising the maximum weighted force transmissibility, opt($J_{T_{F,W}}$) and minimising the maximum weighted time-averaged power transmission to the hull, opt($J_{\langle \Pi_W \rangle}$). The opt($J_{T_{F,W}}$) and opt($J_{\langle \Pi_W \rangle}$) parameter sets for a single RC configuration are given in Table 5. Fig. 6 shows the weighted force transmissibility, $T_{F,W}$, versus frequency for the case without the RC, and using the opt($J_{T_{F,W}}$) and opt($J_{\langle \Pi_W \rangle}$) parameter sets. The largest peak in the response occurring at approximately 55 Hz can be attributed to the fundamental propeller-shafting resonance, while the peaks at around 22, 46 and 73 Hz are due to excitation of hull axial resonances. The introduction of the RC results in the elimination of the dominant propeller-shafting resonance and introduces another resonance at approximately 16 Hz, as well as significantly lowering the maximum response. It can be seen however that the opt($J_{\langle \Pi_W \rangle}$) parameter set does not correlate to the optimum parameter set obtained when minimising the maximum weighted force transmissibility, $J_{T_{F,W}}$. A plot of the weighted time-averaged power transmission to the hull, $\langle \Pi_W \rangle$, versus frequency is presented in Fig. 7, again without the RC, and using the opt($J_{T_{F,W}}$) and opt($J_{\langle \Pi_W \rangle}$) parameter sets. This figure displays the same resonances as Fig. 6, however in this case the hull resonances are more significant in amplitude. Similar to Fig. 6, Fig. 7 shows that the opt($J_{T_{F,W}}$) parameter set does not result in the minimal $\langle \Pi_W \rangle$ controlled response. It was observed that optimisation of $T_{F,W}$ using the opt($J_{T_{F,W}}$) parameter set and $\langle \Pi_W \rangle$ using the opt($J_{\langle \Pi_W \rangle}$) parameter set using a single RC results in the two largest resonance peaks in the controlled responses becoming equal. It was observed that a smaller virtual mass increases the effective bandwidth of the response which is attenuated (that is, the suppression band). This result is contrary to the traditional DVA which demonstrates a widening of the suppression band with an increase in the DVA mass. The increase in the suppression band for a smaller virtual mass is due to the inertial force associated with the RC being proportional to the relative motion of its two opposing terminals. Increasing the virtual mass increases the impedance between the RC terminals. In the upper limit, an infinite virtual mass would reduce the RC dynamically to a rigid link.

The opt($J_{T_{F,W}}$) and opt($J_{\langle \Pi_W \rangle}$) parameter sets for a dual RC configuration consisting of two RCs in series are given in Table 6. Figs. 8 and 9, respectively, present $T_{F,W}$ and $\langle \Pi_W \rangle$ versus frequency for the dual RC configuration, each showing the uncontrolled response and the controlled responses obtained using the two

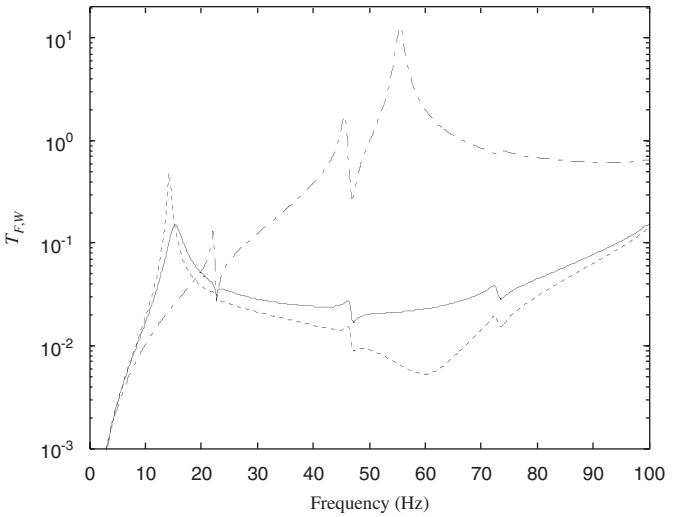

Fig. 6. Log weighted force transmissibility of the propeller-shafting system: without the RC (– – -), with the RC tuned to minimise $T_{F,W}$ (——) and with the RC tuned to minimise $\langle \Pi_W \rangle$ (- - - - -).

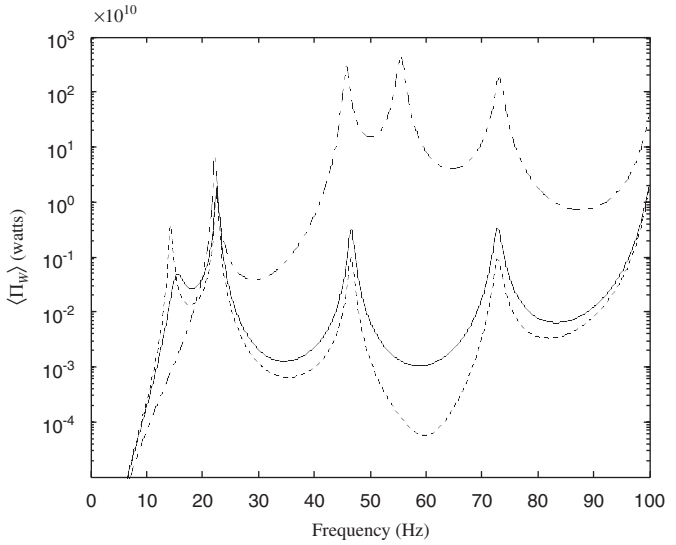

Fig. 7. Log weighted time-averaged power transmission to the propeller-shafting system: without the RC (– – -), with the RC tuned to minimise $T_{F,W}$ (——) and with the RC tuned to minimise $\langle \Pi_W \rangle$ (- - - - -).

Table 6
Optimal parameters for a dual RC configuration

RC parameter	Opt($J_{T_{F,W}}$)	Opt($J_{\langle \Pi_W \rangle}$)
$k_{r,1}$ (MN/m)	116.91	93.192
$m_{r,1}$ (tonnes)	1	1
$c_{r,1}$ (tonnes/s)	573.32	71.610
$k_{r,2}$ (MN/m)	596.73	1265.6
$m_{r,2}$ (tonnes)	1.7859	3.1525
$c_{r,2}$ (tonnes/s)	134.37	256.16

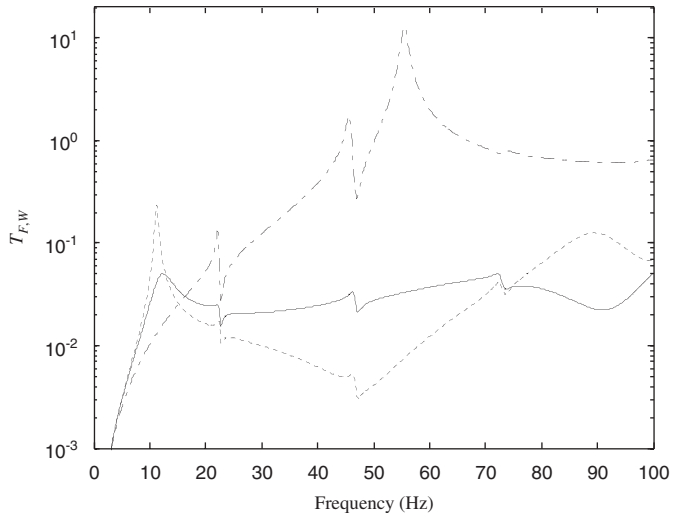

Fig. 8. Log weighted force transmissibility of the propeller-shafting system: without the RC (– - -), with 2 RCs tuned to minimise $T_{F,W}$ (——) and with 2 RCs tuned to minimise $\langle \Pi_W \rangle$ (- - - - -).

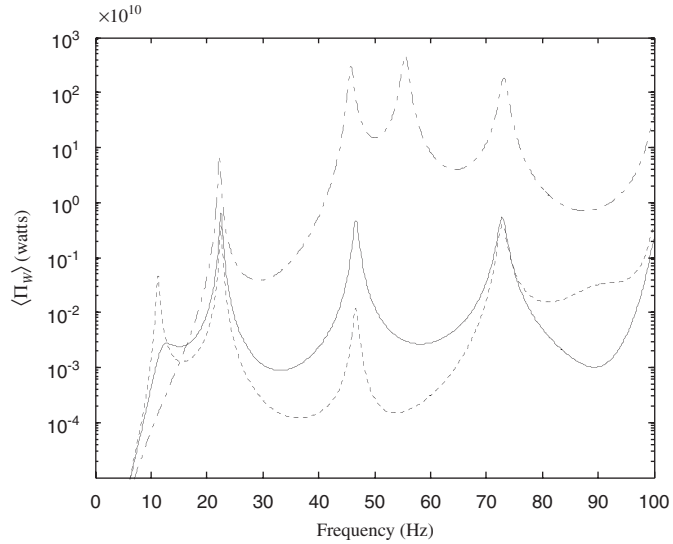

Fig. 9. Log weighted time-averaged power transmission to the propeller-shafting system: without the RC (– - -), with 2 RCs tuned to minimise $T_{F,W}$ (——) and with 2 RCs tuned to minimise $\langle \Pi_W \rangle$ (- - - - -).

fitness functions. These two figures show similar trends to Figs. 6 and 7 with the exception that three dominant peaks in the optimal controlled responses have become equal as a result of the optimisation process. It is of interest to note that one of the three equal peaks in the optimal controlled response for $\langle \Pi_W \rangle$ (Fig. 9) corresponds to the hull resonance occurring at 73 Hz. This demonstrates the importance of including the dynamic response of the hull when tuning the RC parameters.

A comparison of the controlled responses for $T_{F,W}$ obtained using the Goodwin model (for one RC) and the opt($J_{T_{F,W}}$) parameter sets using the single and dual RC configurations is shown in Fig. 10. Similarly, a comparison of the controlled responses for $\langle \Pi_W \rangle$ obtained using the Goodwin model (one RC) and the opt($J_{\langle \Pi_W \rangle}$) parameter sets using one and two RCs in series is presented in Fig. 11. Both figures show that the controlled response obtained using the dual RC configuration results in the lowest peak, while the Goodwin

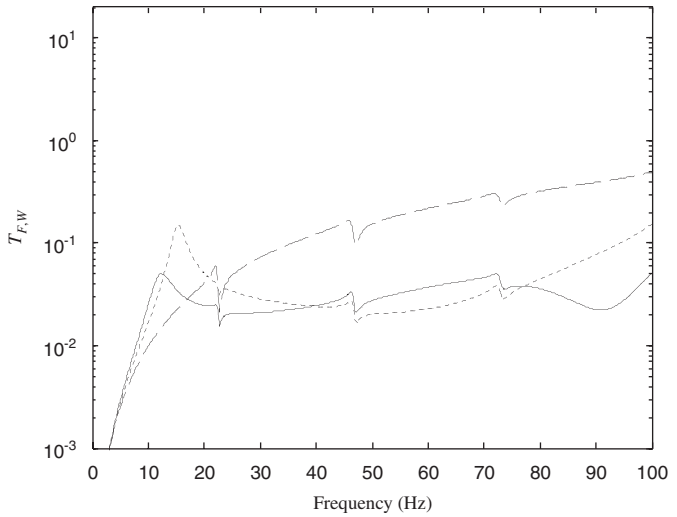

Fig. 10. Log weighted force transmissibility of the propeller-shafting system: optimal RC using Goodwin's method (– - -), with 1 RC tuned to minimise $T_{F,W}$ (- - - - -) and with 2 RCs tuned to minimise $T_{F,W}$ (——).

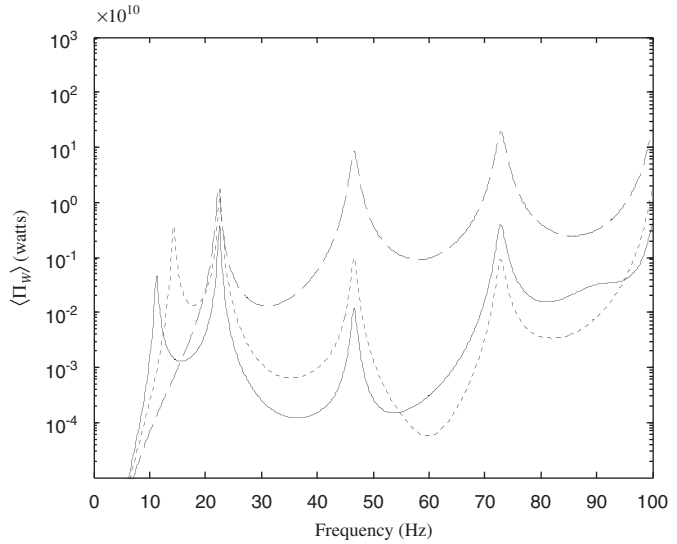

Fig. 11. Log weighted time-averaged power transmission to the propeller-shafting system: optimal RC using Goodwin's method (– - -), with 1 RC tuned to minimise $\langle \Pi_W \rangle$ (- - - - -) and with 2 RCs tuned to minimise $\langle \Pi_W \rangle$(——).

parameter set results in the worst controlled response over the frequency range of interest. This information is presented graphically in Fig. 12 in terms of a percentage reduction of the maximum response (relative to the uncontrolled response in the absence of a RC) for all the parameter sets. Fig. 12 clearly shows that the opt($J_{\langle \Pi_W \rangle}$) parameter sets for both one or two RC configurations achieves significant reduction in $\langle \Pi_W \rangle$, but has a poor $T_{F,W}$ response compared with the other parameter sets. In contrast, the opt($J_{T_{F,W}}$) parameter sets using one and two RCs results in excellent reduction of both the $T_{F,W}$ and $\langle \Pi_W \rangle$ responses.

It is of interest to perform a perturbation analysis in order to observe the effect of any variations in the system parameters from an idealised case. A general procedure for studying the parameter sensitivities could be used to assess the change in the system's response to variations in the RC parameters. However due to the sufficiently large modal spacing, discrete variations on the RC parameters of $\pm 10\%$ is regarded to be adequate for the perturbation analysis considered within this work. In this investigation, perturbations of the thrust

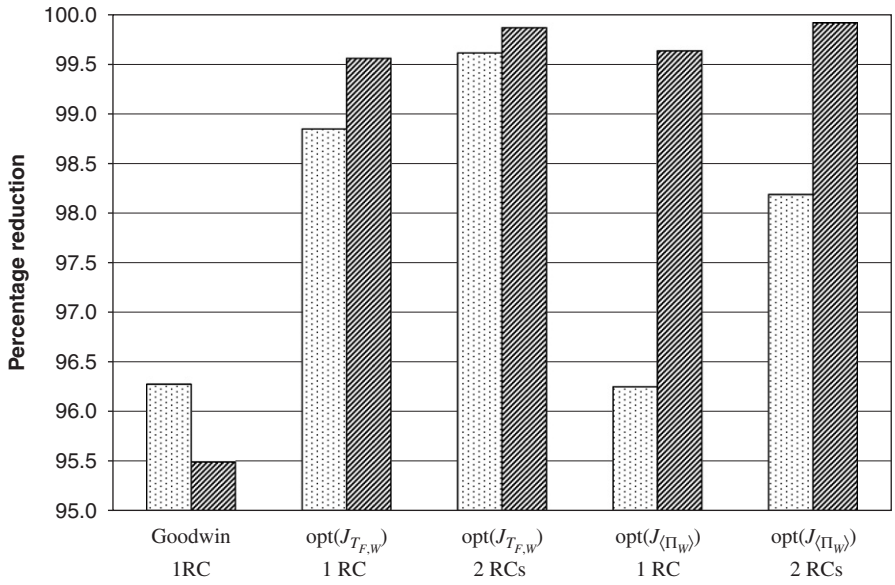

Fig. 12. Percent reduction in the response for the various parameter sets relative to the response without the RC: $T_{F,W}$, $\langle \Pi_W \rangle$.

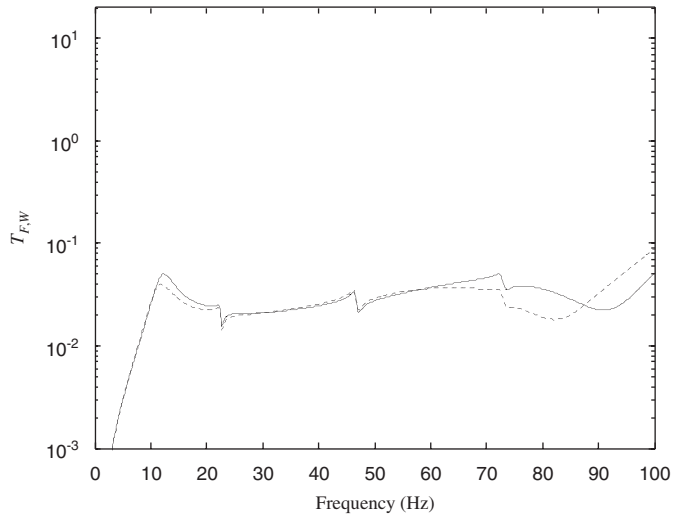

Fig. 13. Log weighted force transmissibility of the propeller-shafting system: with 2 RCs tuned to minimise $T_{F,W}$ (——) and with 2 perturbed RCs tuned to minimise $T_{F,W}$ (- - - - -).

bearing and RC parameters have been considered. The thrust bearing was chosen since its dynamic properties are nonlinear and vary considerably within its operating range [1]. It was found however that major perturbations provided insignificant changes in both the $T_{F,W}$ and $\langle \Pi_W \rangle$ responses. This is due to the large stiffness and low mass of the thrust bearing relative to the other propeller-shafting system components. Figs. 13 and 14, respectively, show the controlled responses for $T_{F,W}$ and $\langle \Pi_W \rangle$ using two RCs in series. In each figure, the optimal controlled response is shown as well as the controlled response obtained by perturbing the optimal RC parameters by ±10%. All combinations of the perturbation quantities (by ±10%) on the RC parameters were considered and the combination which resulted in the worst-case scenario (largest increase in

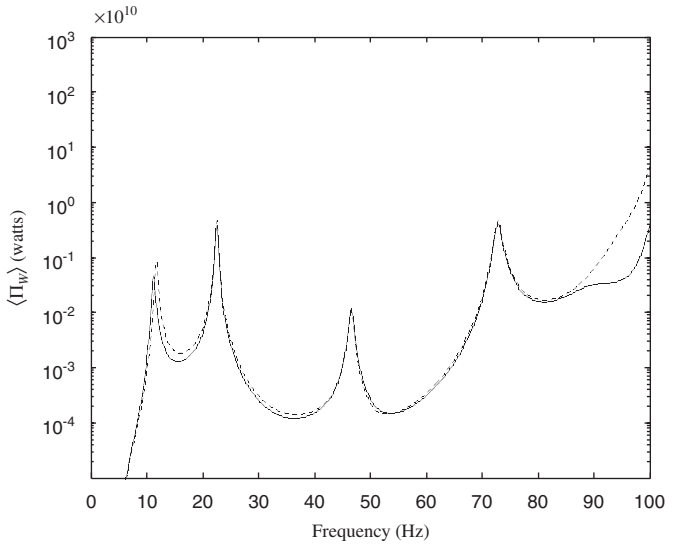

Fig. 14. Log weighted time-averaged power transmission to the propeller-shafting system: with 2 RCs tuned to minimise $\langle \Pi_W \rangle$ (——) and with 2 perturbed RCs tuned to minimise $\langle \Pi_W \rangle$ (- - - - -).

Table 7
Percentage perturbations on RC parameters

RC parameter	opt($J_{T_{F,W}}$) (%)	opt($J_{\langle \Pi_W \rangle}$) (%)
$k_{r,1}$ (MN/m)	−10	+10
$m_{r,1}$ (tonnes)	+10	+10
$c_{r,1}$ (tonnes/s)	+10	−10
$k_{r,2}$ (MN/m)	−10	+10
$m_{r,2}$ (tonnes)	+10	−10
$c_{r,2}$ (tonnes/s)	+10	−10

the controlled response) is given in Table 7. Results showed that perturbations in the RC parameters did not significantly affect either the $T_{F,W}$ and $\langle \Pi_W \rangle$ controlled responses.

5. Conclusions

The dynamic response of the propeller-shafting system in a submarine has been modelled using a modular transmission matrix description allowing for flexibility in future design modifications. Both propeller-shafting and hull resonances were present when examining the force transmissibility and power transmission to the hull, which demonstrates the importance of including the hull in the dynamic modelling. Optimal RC parameters have been obtained by minimising the frequency weighted maximum force transmissibility and time-averaged power transmission to the submarine hull over a specified frequency range. An optimisation scheme using a genetic and a general nonlinear constrained algorithm was applied to the fitness criteria for single and dual RC configurations. Realistic lower and upper bounds on the RC parameters were applied as constraints within the optimisation process. It was shown that minimisation of the power transmission does not necessarily provide the minimum force transmissibility. Perturbations of the thrust bearing and resonance changer parameters were shown to have no significant effect on the controlled responses.

References

[1] J. Pan, N. Farag, T. Lin, R. Juniper, Propeller induced structural vibration through the thrust bearing, *Proceedings of Acoustics 2002*, Adelaide, Australia, 13–15 November 2002, pp. 390–399.
[2] A.J.H. Goodwin, The design of a resonance changer to overcome excessive axial vibration of propeller shafting, *Institute of Marine Engineers—Transactions* 72 (1960) 37–63.
[3] D.W. Lewis, P.E. Allaire, P.W. Thomas, Active magnetic control of oscillatory axial shaft vibrations in ship shaft transmission systems, part 1: system natural frequencies and laboratory scale model, *Tribology Transactions* 32 (1989) 170–178.
[4] H. Frahm, 1911 US Patent 989,958, Device for damping vibrations of bodies.
[5] J.B. Hunt, *Dynamic Vibration Absorbers*, Mechanical Engineering Publications LTD, London, 1979.
[6] B.G. Korenev, L.M. Reznikov, *Dynamic Vibration Absorbers Theory and Technical Applications*, Wiley, Chichester, 1993.
[7] D. Hartog, *Mechanical Vibrations*, McGraw-Hill, New York, 1956.
[8] V.H. Neubert, Dynamic absorbers applied to a bar that has solid damping, *Journal of the Acoustical Society of America* 36 (1964) 673–680.
[9] L. Kitis, B.P. Wang, W.D. Pilkey, Vibration reduction over a frequency range, *Journal of Sound and Vibration* 89 (1983) 559–569.
[10] A.H.P. Lau, G.C.K. Lam, The optimal design of dynamic absorber in the time domain and the frequency domain, *Journal of Applied Acoustics* 28 (1989) 67–78.
[11] H.J. Rice, Design of multiple vibration absorber systems using modal data, *Journal of Sound and Vibration* 160 (1993) 378–385.
[12] D.A. Rade, V.J. Steffen, Optimisation of dynamic vibration absorbers over a frequency band, *Journal of Sound and Vibration* 14 (2000) 679–690.
[13] J.C. Snowdon, Mechanical four-pole parameters and their application, *Journal of Sound and Vibration* 15 (1971) 307–323.
[14] S. Rubin, Mechanical immittance and transmission-matrix concepts, *Journal of the Acoustical Society of America* 41 (1966) 1171–1179.
[15] R.E.D. Bishop, D.C. Johnson, *The Mechanics of Vibration*, Cambridge University Press, Cambridge, 1960.
[16] W.C.L. Hu, D.D. Kana, Four-pole parameters for impedance analysis of conical and cylindrical shells under axial excitations, *Journal of the Acoustical Society of America* 43 (1968) 683–690.
[17] E. Skudrzyk, *Simple and Complex Vibratory Systems*, The Pennsylvania State University Press, London, 1968.
[18] A. Osyczka, *Evolutionary Algorithms for Single and Multicriteria Design Optimization*, Physica-Verlag, New York, 2002.
[19] D.E. Goldberg, *Genetic Algorithms in Search, Optimization and Machine Learning*, Addison-Wesley, Reading, MA, 1989.
[20] F. Erbatur, I. Hassancebi, I. Tutuncu, H. Kilic, Optimal design of planar and space structures with genetic algorithms, *Computers and Structures* 75 (2000) 209–224.